

# p38 mitogen-activated protein kinase gene silencing rescues rat hippocampal neurons from ketamine-induced apoptosis: An *in vitro* study

XIAO-QIAN GUO<sup>\*</sup>, YU-LING CAO<sup>\*</sup>, LI ZHAO, XUAN ZHANG, ZHONG-RUI YAN and WEI-MEI CHEN

Department of Neurology, Jining No. 1 People's Hospital, Jining, Shandong 272011, P.R. China

Received November 19, 2017; Accepted June 26, 2018

DOI: 10.3892/ijmm.2018.3750

**Abstract.** Ketamine (KTM) is an anesthetic drug with several advantages, including the elevation of cardiac output and blood pressure. However, KTM may also induce the apoptosis of hippocampal neurons. Notably, p38 mitogen-activated protein kinase (p38MAPK) has previously been studied for its role in neuronal injury. Therefore, the present study evaluated the effect of lentivirus-mediated p38MAPK gene silencing on KTM-induced apoptosis of rat hippocampal neurons. Hippocampal neurons were extracted from neonatal Sprague-Dawley rats, and then treated with KTM, p38MAPK-short hairpin RNA or SB203580 (an inhibitor of p38MAPK). Next, the expression levels of p38MAPK and apoptosis-associated genes, including caspase-3, B-cell lymphoma 2 (Bcl-2) and Bcl-2-associated X protein (Bax), were detected. In addition, cell viability and apoptosis were determined using an MTT assay and flow cytometry, respectively. Finally, telomerase activity of hippocampal neurons was detected by ELISA. The results revealed that silencing of p38MAPK in KTM-treated cells decreased the expression levels of p38MAPK, caspase-3 and Bax, and the extent of p38MAPK phosphorylation, while it increased the expression of Bcl-2. Furthermore, silencing p38MAPK promoted cell viability, cell cycle progression and the telomerase activity of hippocampal neurons, and inhibited the apoptosis of hippocampal neurons. Taken together, the results suggested an inhibitory role of lentivirus-mediated p38MAPK gene silencing on KTM-induced apoptosis of rat hippocampal neurons. Thus, p38MAPK gene silencing may serve as a potential target for preventing the KTM-induced apoptosis of hippocampal neurons.

## Introduction

Ketamine (KTM) is an important drug for inducing anesthesia that is used for sedation, as well as for relieving pain, and is also applied to facilitate psychological treatments due to its psychedelic nature (1-3). KTM is often used to induce anesthesia in patients at high risk, due to its hemodynamic stability, the absence of respiratory depression, wide therapeutic range and short half-life (4,5). In addition, KTM robustly elevates both cardiac output and blood pressure (6). Studies by Mulvey *et al* (7,8) have reported the safety and efficacy of KTM, which serves as the first choice of anesthetic drug for injury caused by natural disasters. However, patients recovering from KTM anesthesia usually experience several undesirable symptoms, including delirium, hallucination, confusion, and sometimes a feeling of being 'outside of their body' or 'near-death.' Furthermore, KTM can cause excitotoxic damage and neurotoxicity in the fragile neonatal brain (1,9,10), and is also reported to induce apoptosis and necrosis in neuronal cells in nature (9). Moderate or high doses of KTM result in evident changes in the GABAergic system, which increases the differentiation of hippocampal neurons and causes severe neurotoxicity in the neonatal hippocampus (11,12). The hippocampus is one of the most vulnerable brain regions to numerous types of neurobiological insults (13). Proliferation of these vulnerable hippocampal cells serves an important role in learning and memory processes (14). Moreover, the effects of KTM can be mediated by the regulation of mitogen-activated protein kinase (MAPK) signaling in the hippocampus (15). Excitotoxic and ischemic insults in the hippocampus have been demonstrated to be affected by p38MAPK, and the activation of p38MAPK may be part of a neuroprotective response (16).

p38MAPK activates caspase-3 and regulates diverse cellular functions, including senescence, apoptosis and cell cycle arrest (17). The p38MAPK family is usually stimulated by genotoxic agents, such as KTM and cytokines, mediating stress responses and inflammation (16). KTM can decrease the activity of the p38MAPK-mediated modulating pathway (18). In addition, a number of neurotoxic agents have been demonstrated to induce apoptosis in a variety of neuronal cell preparations mediated by the activation of p38 (19). Several studies have suggested that p38MAPK gene silencing has protective functions against apoptosis of hippocampal neuronal cells (13,18). However, further studies are required,

---

*Correspondence to:* Dr Wei-Mei Chen, Department of Neurology, Jining No. 1 People's Hospital, 6 Jiankang Road, Shizhong, Jining, Shandong 272011, P.R. China  
E-mail: chenwm\_ei@126.com

<sup>\*</sup>Contributed equally

**Key words:** p38 mitogen-activated protein kinase, gene silencing, ketamine, hippocampal neurons, apoptosis

since the exact reasons for anesthesia-induced hippocampal neurodegenerative disorders or memory loss remain largely unknown (12). Furthermore, the role of p38MAPK gene silencing in KTM-induced apoptosis in hippocampal neurons has not been fully elucidated. Therefore, the present study investigated the specific mechanisms of p38MAPK gene silencing on KTM-induced apoptosis of rat hippocampal neurons in order to provide a theoretical foundation for the discovery of new therapeutic targets.

## Materials and methods

**Ethics statement.** All animal experimentation conducted in the current study was approved by the Animal Ethics Committee of Jining No. 1 People's Hospital (Jining, China) and abided by relevant protocols. The environmental conditions of the facilities were in accordance with the 'Laboratory Animal-Requirements of Environment and Housing Facilities' guidelines (regulation no. GB14925-2001). All animal breeding and experimental procedures were performed in accordance with protocols issued by the 'Animal Management Regulations' and the Association for Assessment and Accreditation of Laboratory Animal Care International.

**Cell extraction and culture.** A total of 10 neonatal Sprague-Dawley (SD) rats [3-days-old; 8-10 g; Shanghai SLAC Laboratory Animal Co., Ltd., Shanghai, China; production license no. SCXK (Hu) 2012-0002] were sacrificed by cervical dislocation and then sterilized using 75% ethanol. The skin and skull of the rats were dissected to expose bilateral cerebral hemispheres. After the cerebral cortex was separated using an ophthalmic tweezer, the bilateral hippocampal tissues were extracted. The tissues were centrifuged at 130 x g at 4°C for 5 min, and the supernatant was discarded. Following digestion with Accutase enzyme (Sigma-Aldrich; Merck KGaA, Darmstadt, Germany) three times the volume of the hippocampal tissues, the hippocampal tissues were added to Dulbecco's modified Eagle's medium (DMEM; Solarbio Science & Technology Co., Ltd., Shanghai, China) containing 10% fetal bovine serum (FBS; Sijiqing Biological Engineering Materials Co., Ltd., Hangzhou, China), and penicillin (100 U/ml) and streptomycin (100 µg/ml) (North China Pharmaceutical Group Corp. Shijiazhuang, China), and triturated into a cell suspension. The cell suspension was then filtered by a 200-mesh copper sieve, and the filtered cell suspension underwent a centrifugation (4°C; 200 x g) for 10 min with the supernatant discarded and was subsequently added into DMEM/F12 high-glucose medium containing 10% FBS, penicillin (100 U/ml) and streptomycin (100 µg/ml) at 37°C with 5% CO<sub>2</sub>. Hippocampal neurons in the logarithmic growth phases were detached in 0.25% trypsin (Solarbio Science & Technology Co., Ltd.) for preparation of the cell suspension. Following cell counting using a blood cell counting chamber, the cells were seeded in a 6-well plate (Corning Inc., Corning, New York, USA) at a density of 1x10<sup>5</sup>/well for subsequent experiments.

**Cell observation and identification.** Neurons were seeded to a 6-well plate containing coverslips precoated with lysine (Sigma-Aldrich; Merck KGaA). The plate was then transferred

to an incubator with 5% CO<sub>2</sub> at 37°C. After 72 h of culture, a DMEM/F12 containing 10% FBS was added to the plate in replace of the old medium, followed by the addition of 10 mol/l arabinoside (Jun Rui Biotechnology, Shanghai, China). At days 3, the medium was changed and the arabinoside was removed. Cell morphology and growth were observed under an inverted phase contrast microscope (Olympus Corp., Tokyo, Japan) at days 1, 3, 7 and 21. Neurons at 7 days of culture were collected with a micropipette, washed with PBS three times (5 min each time), fixed with 4% paraformaldehyde for 15 min at room temperature, and then washed with PBS for a further three times. Neurons were cultured with mouse anti-rat class III β-tubulin primary antibody (AT809, 1:250; Beyotime Institute of Biotechnology, Shanghai, China) in a wet box (containing wet filter paper) at 4°C for 12 h, in order to prevent the coverslips from being dry. Neurons were then washed with 1% PBS containing Tween-20 (PBST) three times (5 min each time), incubated with fluorescein isothiocyanate (FITC)-labeled goat anti-rabbit secondary IgG antibody (1:400; Jackson Laboratory, Bar Harbor, ME, USA) at 37°C for 1 h in the dark and washed with 1% PBST three times (5 min each time). Neurons were incubated in 5 µg/ml Hoechst 33342 (Sigma-Aldrich; Merck KGaA) for 10 min at room temperature. Neurons were treated with a quenching agent subsequent to washing with PBST five times (5 min each time), and then activated by ultraviolet rays at an excitation and an emission wavelength of 346 and 448 nm, respectively. Images of the fluorescence staining of neurons and nuclei were captured and observed under a high-power microscope.

**Construction of the p38MAPK-short hairpin RNA (shRNA) lentivirus vector.** Both ends of positive and negative strand templates in an shRNA targeting p38MAPK (SABioscience; Qiagen GmbH, Hilden, Germany) were annealed following the addition of *Bam*HI (GGATCC) and *Eco*RI (GAATTC), respectively. The shRNA template was then subcloned into the pLL3.7 vector, which had been linearized by *Bam*HI and *Eco*RI. Subsequent to screening, enzyme digestion, identification and sequencing performed by Sangon Biotech Co., Ltd. (Shanghai, China), the p38MAPK-shRNA was obtained. The lentivirus shuttle plasmid and auxiliary packaging vector plasmid DNA solution were prepared using the following procedure: Interference plasmids (10 µg pRsv-REV, 15 µg pMDlg-Prre, 7.5 µg pMD2G and 20 µg p38MAPK-shRNA) were mixed, and sterile water was added until a constant volume of 1,800 µl was obtained. Next, 200 µl CaCl<sub>2</sub> (2.5 mol/l) was added and mixed evenly, followed by addition of 2,000 µl borate buffered saline (2X). The sample was kept at room temperature for 20-30 min, and then 293T cells (American Type Culture Collection, Manassas, VA, USA) were transfected at 80-90% density. Subsequently, the culture liquid containing monolayer cells was mixed uniformly with the pRsv-REV, pMDlg-Prre, pMD2G and p38MAPK-shRNA plasmids and calcium phosphate as the transfection reagent, and the medium was replaced with a complete medium at 8 h after transfection. Following transfection for 48 h, the supernatant with lentivirus particles was collected, centrifuged at 500 x g at 4°C for 10 min to remove shedding cells and large cell debris, and then filtered using a 0.45 µm polyvinylidene fluoride membrane. The lentivirus supernatant was added to

an ultra-clear SW28 centrifugation tube (Beckman Coulter Life Sciences, Brea, CA, USA), followed by centrifugation at 4°C at 900 x g for 2 h. PBS was used to rinse the precipitates, which were then dissolved at 4°C, followed by centrifugation at 500 x g for 1 min. Lastly, the lentivirus supernatant was separately packaged and stored at a -80°C refrigerator for further use.

**Cell transfection and grouping.** Neurons in the logarithmic growth phase were detached prior to transfection, collected and seeded into a 6-well plate. Transfection was performed using lentivirus plasmid when the neurons were at 80-90% confluence. Next, the neurons were randomly grouped into the following groups: KTM group, treated with 2,500  $\mu\text{mol/l}$  KTM; KTM + SB203580 group, treated with 20.0  $\mu\text{mol/l}$  SB203580 (p38MAPK inhibitor, PHZ1253, Invitrogen; Thermo Fisher Scientific, Inc., Waltham, MA, USA) and 2,500  $\mu\text{mol/l}$  KTM solution; KTM + negative control (NC) group, transfected with empty lentivirus plasmid and 2,500  $\mu\text{mol/l}$  KTM solution; KTM + p38MAPK-shRNA group, transfected with p38MAPK-shRNA lentivirus and 2,500  $\mu\text{mol/l}$  KTM solution; and the control group, treated with an equal volume of culture medium. KTM (KH080401; Fujian Gutian Pharmaceutical Co., Ltd., Ningde, China) used in these groups was dissolved in DMEM. After transfection for 48 h, the expression of enhanced green fluorescent protein (EGFP; BioVision, Inc., Milpitas, CA, USA) in the cells was observed under an inverted microscope.

**Reverse transcription-quantitative polymerase chain reaction (RT-qPCR).** Following transfection for 48 h, the total RNA was extracted using the TRIzol one-step method (Invitrogen; Thermo Fisher Scientific, Inc.). The optical density (OD) of total RNA was measured at 260 and 280 nm using an ultra-violet spectrophotometer to obtain the concentration of RNA. The ratio of the OD at these wavelengths was also calculated to determine the purity of RNA. Total RNA (1  $\mu\text{g}$ ) was then reversely transcribed into cDNA using a PrimeScript™ RT-PCR kit (Perfect Real-Time; RR047A; Takara Bio, Inc., Kyoto, Japan). The reaction was conducted at 37°C for 60 min and at 85°C for 5 min. Primers for qPCR were designed by Primer Premier 5.0 software (Premier Biosoft, Palo Alto, CA, USA) and synthesized by Thermo Fisher Scientific, Inc. (Invitrogen), with glyceraldehyde-3-phosphate dehydrogenase (GAPDH) serving as an internal control (Table I). qPCR was performed using a Bio-Rad instrument (cat. no. 10021337; Bio-Rad Laboratories, Inc., Hercules, CA, USA). The One-Step SYBR PrimeScript PLUS RT-PCR Kit (Takara Bio, Inc.) was used to determine gene expression and the reaction system constituted: 5.3  $\mu\text{l}$  2X Taq MasterMix, 1  $\mu\text{l}$  forward primer (5  $\mu\text{M}$ ), 1  $\mu\text{l}$  reverse primer (5  $\mu\text{M}$ ), 1  $\mu\text{l}$  cDNA and 11.7  $\mu\text{l}$  RNase free H<sub>2</sub>O. The reaction conditions were as follows: Pre-denaturation at 95°C for 3 min, denaturation at 95°C for 10 sec, annealing at 60°C for 20 sec, and extension at 72°C for 30 sec (40 cycles). Relative expression of the target genes was calculated using the 2<sup>- $\Delta\Delta\text{C}_q$</sup>  method (20,21).

**Western blot analysis.** Following transfection for 48 h, the total protein was extracted with the addition of radioimmunoprecipitation assay lysis buffer (Beyotime Institute of Biotechnology),

Table I. Primer sequences used in quantitative polymerase chain reaction.

Gene	Primer sequence
p38MAPK	F: 5'-ACATCGTGTGGCAGTGAAGAAG-3' R: 5'-CTTTTGGCGTGAATGATGGA-3'
GAPDH	F: 5'-GCACAGTCAAGGCTGAGAATG-3' R: 5'-ATGGTGGTGAAGACGCCAGTA-3'
Caspase-3	F: 5'-GAGACAGACAGTGGAACTGACA ATG-3' R: 5'-GGCGCAAAGTGACTGGATGA-3'
Bax	F: 5'-AGACACCTGAGCTGACCTTGGAG-3' R: 5'-GTTGAAGTTGCCATCAGCAAACA-3'
Bcl-2	F: 5'-TGAACCGGCATCTGCACAC-3' R: 5'-CGTCTTCAGAGACAGCCAGGAG-3'

p38MAPK, p38 mitogen-activated protein kinase; GAPDH, glyceraldehyde-3-phosphate dehydrogenase; Bcl-2, B-cell lymphoma 2; Bax, Bcl-2-associated X protein; F, forward; R, reverse.

and the concentration of total protein was determined using the bicinchoninic acid assay (KeyGen Biotech Co., Ltd., Nanjing, China). Extracted proteins were mixed with the loading buffer and boiled at 100°C for 5 min. Protein (10  $\mu\text{g}$ ) from each group was then subjected to vertical sodium dodecyl sulfate-polyacrylamide gel electrophoresis (10% SDS-PAGE) and transferred at 250 mA for 45 min to a polyvinylidene fluoride membrane (EMD Millipore, Billerica, MA, USA). Next, the membrane was blocked with 5% skimmed milk in PBST for 1 h at room temperature and incubated overnight at 4°C with GAPDH (ab8245; 1:1,000), p38MAPK (ab31828; 1:1,000), phosphorylated (p)-p38MAPK (ab47363; 1:1,000), caspase-3 (ab2171; 1:500), B-cell lymphoma 2 (Bcl-2; ab32124; 1:1,000) and Bcl-2-associated X protein (Bax; ab32503; 1:1,000; all purchased from Abcam, Cambridge, MA, USA) primary antibodies. The membrane was subsequently washed with TBST four times (5 min each time) prior to the addition of horseradish peroxidase-labeled goat anti-mouse IgG secondary antibody (ab6728; 1:2,000; Abcam) and shaken at 37°C for 1 h. After washing three times with TBST, the membrane was exposed and developed using enhanced chemiluminescence (Pierce; Thermo Fisher Scientific, Inc.), and the film was scanned. A gel documentation system (UVP, LLC, Phoenix, AZ, USA) was used to analyze the OD value of the target bands, and GAPDH served as the internal control.

**MTT assay.** Following transfection for 48 h, neurons were washed two times with PBS, detached by 0.25% trypsin and made into a single cell suspension. Cells in the suspension were counted and seeded into a 96-well plate at a density of 3-6 ( $\times 10^3$ ) cells per well in 200  $\mu\text{l}$  cell-culture medium. Each culture was set-up in triplicate and incubated in a cell culture incubator for 12, 24 and 48 h, respectively. After the different times of incubation, 20  $\mu\text{l}$  of 5 mg/ml MTT (Sigma-Aldrich; Merck KGaA) was added to each well, and then a further 4-h



culture was conducted at 37°C in 5% CO<sub>2</sub>. The supernatant was carefully removed with a syringe, and a total of 150 µl of dimethyl sulfoxide (Amresco, LLC, Solon, OH, USA) was added to each well and oscillated in a horizontal shaker for 10 min to dissolve the crystallization. The OD of each well was measured at 570 nm using a microplate reader (Bio-Rad Laboratories, Inc.). The cell survival rate was calculated according to  $(OD_{\text{experimental group}} - OD_{\text{blank group}})/(OD_{\text{control group}} - OD_{\text{blank group}}) \times 100\%$ , and the cell survival rate of each group was evaluated by comparing it with that of the control group. The experiment was conducted five times.

**Flow cytometry with propidium iodide (PI) staining.** After transfection for 48 h, the cell suspension was prepared by digestion with EDTA-free trypsin and centrifuged at 200 x g at 4°C for 5 min. The supernatant was discarded, and neurons were washed three times with 5% cold PBS and re-suspended in 300 µl 5% PBS after the supernatant was aspirated. Next, the samples were fixed for 12 h in 700 µl 75% absolute ethanol and centrifuged for 5 min (4°C; 800 x g), followed by aspiration of the supernatant. The neurons were then washed with PBS, stained with 1% PI (Invitrogen; Thermo Fisher Scientific, Inc.) containing RNase for 30 min and further washed with PBS, and the volume was adjusted to 1 ml. The cell cycle progression was detected by BD-Aria FACSCalibur flow cytometry (BD Biosciences, San Jose, CA, USA). Each group had three samples and experiments were repeated three times. The cell cycle distribution was analyzed by ModFit software (Bio-Rad Laboratories, Inc.).

**Enzyme-linked immunosorbent assay (ELISA).** A telomerase PCR-ELISA kit (cat. no. 11854666910; Roche Applied Science, Mannheim, German) was used to detect telomerase activity. Neurons in the logarithmic growth phase were seeded into 6-well plates with  $2 \times 10^5$  cells/well. Following incubation for 24 h, cells were rinsed twice with D-Hanks buffer solution and detached by trypsin. Subsequent to centrifugation at 3,000 x g for 10 min at 4°C, the telomerase lysate was added into samples for lysis on ice for 30 min. Next, cells were centrifuged at 16,000 x g for 20 min at 4°C, and the cell supernatant was extracted for repeat sequence amplification reaction as follows: Primer extension at 25°C for 25 min and telomerase inactivation at 94°C for 5 min, followed by PCR amplification with 30 cycles of at 94°C for 30 sec, 50°C for 30 sec and 72°C for 30 sec, and finally, balance at 72°C for 10 min. The PCR amplified products (5 µl) were mixed with denatured reagents (20 µl), and left to stand at the room temperature for 10 min. Subsequently, the hybrid mixture containing digoxin-labeled probes which were complementary to telomeric repeat sequences (225 µl) was added into samples. The product of the aforementioned reaction (100 µl) was hybridized on the microplates covered with biotin protein at 37°C avoiding light. The anti-digoxin antibody of coupling peroxidase (100 µl/well) was added to the samples at the room temperature for 30 min, followed by addition of 3,5,3',5'-tetramethylbenzidine with the substrate of peroxidase for developing for 4 min. The reaction was halted by adding the termination reagent. Subsequently, a microplate reader (Thermo Fisher Scientific, Inc.) was employed in order to detect the OD value at the wavelengths of 450 and 690 nm.

**Flow cytometry with Annexin V-FITC/PI staining.** Subsequent to transfection for 48 h, neurons were detached by EDTA-free trypsin, washed with PBS three times and then centrifuged for 5 min (4°C, 800 x g). The supernatant was aspirated, and the cell suspension (100 µl) suspended in moderate binding buffer was selected in a 5-ml flow tube. Annexin V-FITC/PI (1:2:50) was then added according to the protocol of the Annexin V-FITC/PI apoptosis detection kit (M3021; Shanghai Meiji Biotechnology Co., Ltd., Shanghai, China). Neurons ( $1 \times 10^6$  cells) were resuspended in 100 µl staining solution, mixed uniformly and stained for 15 min at room temperature in the dark. FITC fluorescence was detected at 510-nm and PI fluorescence at 620-nm bandpass filters, respectively, which were activated at an excitation wavelength of 488 nm using a flow cytometer. Apoptosis in neurons was determined as follows: Dead cells were represented in the upper left quadrant, negative normal cells were in the lower left quadrant, late apoptotic cells were in the upper right quadrant and early apoptotic cells were in the lower right quadrant.

**Statistical analysis.** Statistical analyses were conducted using SPSS version 21.0 software (IBM Corp., Armonk, NY, USA). Measurement data are expressed as the mean  $\pm$  standard deviation. Means between groups were compared by t-test. Multiple groups were compared by one-way analysis of variance after the homogeneity of variance test. Pairwise comparisons among multiple groups were analyzed by the least significant difference t-test.  $P < 0.05$  was considered to be an indicator of a statistically significant difference.

## Results

**Morphological changes of hippocampal neurons treated with KTM, and EGFP expression in the transfected hippocampal neurons.** The morphology and growth conditions of rat hippocampal neurons were observed under a phase contrast inverted microscope at days 0, 1, 3, 7 and 21 (Fig. 1A). After inoculation of hippocampal neurons in neonatal rats (day 0), most cells adhered, presented a round shape and were surrounded by halo; a few cells also protruded. At day 1 after transfection, the neurons grew well with different protrusion lengths and spindle morphology in the majority of cells, whereas no clear connection was established between neurons. After transfection for 3 days, cell protrusions increased, cells were evidently elongated and thickened, and connections between neurons began to form. The neurons were plump, and there was a halo around them. After transfection for 7 days, neurons were plumper, while the halo around the neurons was more visible, and cell protrusions appeared more often and were longer. Neurons moved closer to each other and began to form cell populations, and cell protrusions formed a dense nerve fiber network. After transfection for 21 days, the degeneration of neurons, pyknosis and fragmentation of nuclei were evident. Cell protrusions were reduced in size and severed, and the halo around the cells faded.

Neurons were also observed under a laser scanning confocal microscope (LSCM) using immunofluorescence staining (Fig. 1B). The cytoplasm and protuberance of positive neurons appeared green, and nuclei were stained blue. A total of five visual fields were randomly selected. The

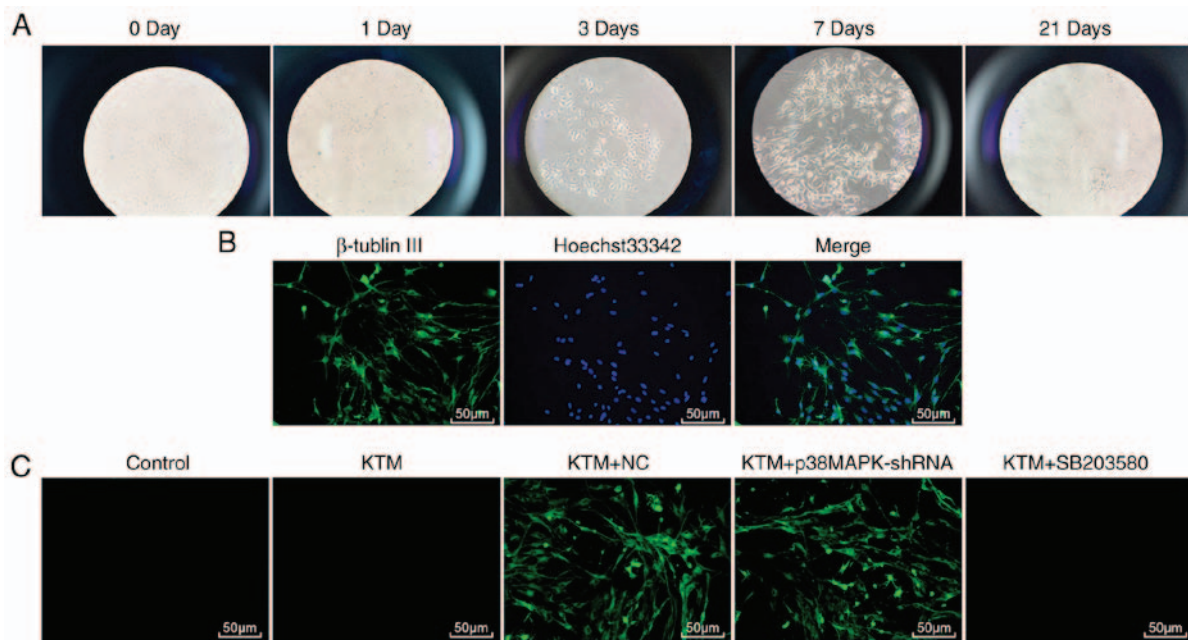


Figure 1. Morphological changes, purity and transfection efficiency of the hippocampal neurons and EGFP expression in the transfected hippocampal neurons (magnification x200). (A) Morphology of hippocampal neurons subsequent to transfection for 0, 1, 3, 7 and 21 days. (B) Purity of rat hippocampal neurons stained with  $\beta$ -tubulin III and Hoechst 33342. (C) Identification of neuron transfection efficiency. KTM, ketamine; NC, negative control; p38MAPK, p38 mitogen-activated protein kinase; shRNA, short hairpin RNA; EGFP, enhanced green fluorescent protein.

purity of neurons was identified as  $92.1 \pm 2.9\%$ . Subsequently, the neuron transfection efficiency was detected. After transfection for 48 h, the EGFP expression clearly increased, with  $>75\%$  cells exhibiting green fluorescence. Furthermore, the neuron transfection efficiency in the KTM + NC and KTM + p38MAPK-shRNA groups was 76 and 79%, respectively (Fig. 1C).

*Silencing p38MAPK decreases the mRNA expression levels of p38MAPK, caspase-3 and Bax, and increases Bcl-2 mRNA expression.* RT-qPCR was employed to measure the mRNA expression levels of p38MAPK, caspase-3, Bax and Bcl-2 in rat hippocampal neurons among the five groups. According to the results of RT-qPCR, in the KTM and KTM + NC groups, the mRNA expression levels of p38MAPK, caspase-3 and Bax were elevated, while Bcl-2 was reduced, as compared with the control group (all  $P < 0.05$ ). In the KTM + SB203580 and KTM + p38MAPK-shRNA groups, the mRNA expression of p38MAPK exhibited no significant difference compared with the control group, while the mRNA levels of caspase-3 and Bax were markedly elevated and Bcl-2 significantly declined (all  $P < 0.05$ ). In comparison with the KTM group, the KTM + p38MAPK-shRNA and KTM + SB203580 groups exhibited a markedly downregulated p38MAPK, caspase-3 and Bax expression, and an upregulated Bcl-2 expression (all  $P < 0.05$ ; Fig. 2). These findings revealed that silencing p38MAPK decreases the mRNA expression levels of p38MAPK, caspase-3 and Bax, and increases Bcl-2 mRNA expression in cells treated with KTM.

*Silencing p38MAPK decreases the protein levels of p38MAPK, caspase-3 and Bax, and increases Bcl-2 protein expression.* Western blot analysis was employed to measure

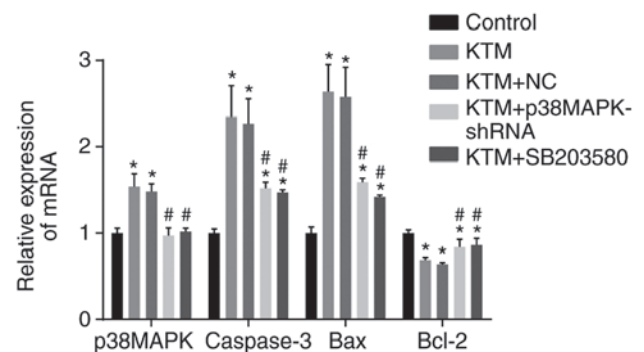


Figure 2. Reverse transcription-quantitative polymerase chain reaction demonstrates that silencing p38MAPK in KTM-induced cells decreases the mRNA expression levels of p38MAPK, caspase-3 and Bax, and increases Bcl-2 mRNA expression. \* $P < 0.05$  vs. the control group; # $P < 0.05$  vs. the KTM group. KTM, ketamine; NC, negative control; p38MAPK, p38 mitogen-activated protein kinase; shRNA, short hairpin RNA; Bcl-2, B-cell lymphoma 2; Bax, Bcl-2-associated X protein.

the protein expression levels of p38MAPK, caspase-3, Bax and Bcl-2, as well as the extent of p38MAPK phosphorylation, in rat hippocampal neurons among the five groups. As demonstrated by the results of this analysis in Fig. 3, compared with the control group, the KTM and KTM+NC groups exhibited increased protein expression levels of p38MAPK, p-p38MAPK, caspase-3 and Bax, and decreased expression of Bcl-2 (all  $P < 0.05$ ). In the KTM + SB203580 and KTM + p38MAPK-shRNA groups, the levels of p38MAPK and p-p38MAPK protein showed no significant difference compared with the control group ( $P > 0.05$ ), while the expression levels of caspase-3 and Bax were markedly increased and Bcl-2 evidently decreased (all  $P < 0.05$ ). Compared with the KTM group, the KTM + p38MAPK-shRNA and KTM + SB203580

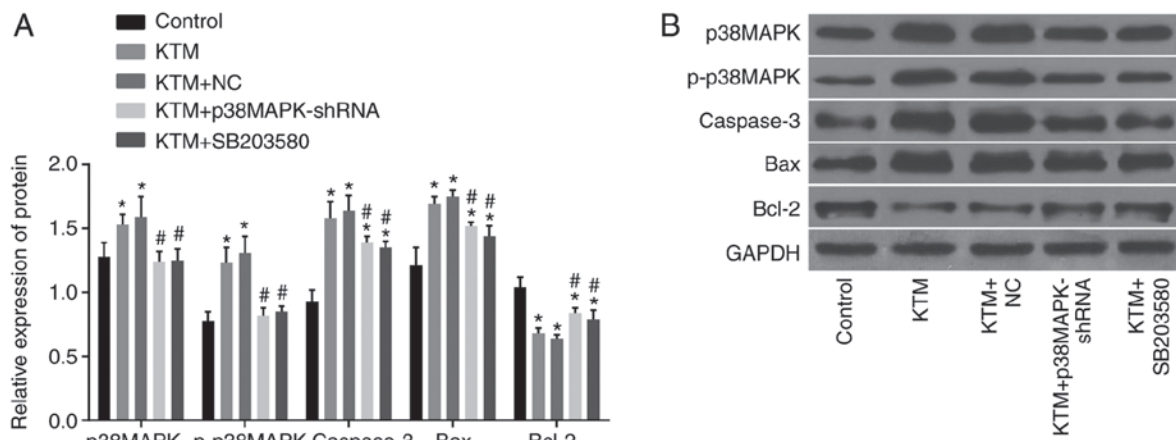


Figure 3. Western blot analysis demonstrates that silencing p38MAPK decreases the protein expression levels of p38MAPK, caspase-3 and Bax, and the extent of p38MAPK phosphorylation, while it increases Bcl-2 protein expression. (A) Relative protein expression in each group following transfection, as detected by western blot analysis. (B) Gray value of associated proteins in each group following transfection. \* $P < 0.05$  vs. the control group; # $P < 0.05$  vs. the KTM group. KTM, ketamine; NC, negative control; p38MAPK, p38 mitogen-activated protein kinase; p-, phosphorylated; shRNA, short hairpin RNA; GAPDH, glyceraldehyde-3-phosphate dehydrogenase; Bcl-2, B-cell lymphoma 2; Bax, Bcl-2-associated X protein.

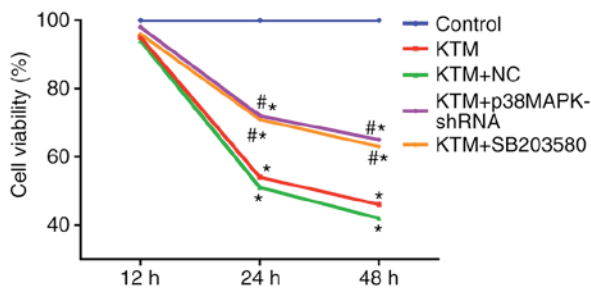


Figure 4. MTT assay demonstrates that silencing p38MAPK promotes cell viability of hippocampal neurons. \* $P < 0.05$  vs. the control group; # $P < 0.05$  vs. the KTM group. KTM, ketamine; NC, negative control; p38MAPK, p38 mitogen-activated protein kinase; shRNA, short hairpin RNA.

groups displayed significantly decreased protein levels of p38MAPK, p-p38MAPK, caspase-3 and Bax, and increased Bcl-2 protein expression (all  $P < 0.05$ ). These findings revealed that silencing p38MAPK decreases the protein expression levels of p38MAPK, caspase-3 and Bax, and increases Bcl-2 protein expression in cells treated with KTM.

**Silencing p38MAPK promotes hippocampal neuron viability.** An MTT assay was used to detect hippocampal neuron viability. As shown in Fig. 4, compared with the control group, the hippocampal neuron viability was notably decreased after 24 h in the KTM, KTM+NC, KTM + SB203580 and KTM + p38MAPK-shRNA groups (all  $P < 0.05$ ). In the KTM + SB203580 and KTM + p38MAPK-shRNA groups, the hippocampal neuron viability significantly increased after 24 h compared with the KTM group (all  $P < 0.05$ ). The results indicated that silencing p38MAPK promotes the viability of hippocampal neurons treated with KTM.

**Silencing p38MAPK promotes cell cycle progression of hippocampal neurons.** Flow cytometry with PI staining was performed to detect the cell cycle distribution of hippocampal neurons. As shown in Fig. 5, compared with the

control group, neurons arrested in the  $G_0/G_1$  phase and their percentage in S phase was evidently decreased in the KTM, KTM+NC, KTM + SB203580 and KTM + p38MAPK-shRNA groups (all  $P < 0.05$ ). In the KTM + p38MAPK-shRNA and KTM + SB203580 groups, the proportion of hippocampal neurons arrested in  $G_0/G_1$  phase was decreased, while it was increased in S phase, compared with the KTM group (all  $P < 0.05$ ). There was no significant difference in the neuronal rate in  $G_2/M$  phase between the five groups (all  $P > 0.05$ ). These findings indicated that silencing p38MAPK promotes cell cycle progression of hippocampal neurons treated with KTM.

**Silencing p38MAPK promotes telomerase activity of hippocampal neurons.** The telomerase activity of hippocampal neurons was detected by ELISA. Compared with the control group, the telomerase activity of hippocampal neurons significantly decreased in the other four groups (all  $P < 0.05$ ). Compared with the KTM group, the KTM + p38MAPK-shRNA and KTM + SB203580 groups displayed increased telomerase activity of hippocampal neurons (both  $P < 0.05$ ), while the KTM+NC group exhibited no significant difference ( $P > 0.05$ ; Fig. 6). These findings implied that silencing p38MAPK promotes the telomerase activity of hippocampal neurons treated with KTM.

**Silencing p38MAPK inhibits apoptosis of hippocampal neurons.** Flow cytometry with Annexin V-FITC/PI staining was performed to detect the apoptosis of hippocampal neurons. As shown in Fig. 7, following incubation for 48 h, the apoptosis rate of rat hippocampal neurons increased in the KTM, KTM+NC, KTM + SB203580 and KTM + p38MAPK-shRNA groups compared with that in the control group (all  $P < 0.05$ ). In comparison with the KTM group, the KTM + p38MAPK-shRNA and KTM + SB203580 groups exhibited a decreased apoptosis rate of rat hippocampal neurons (all  $P < 0.05$ ). These findings implied that silencing p38MAPK suppresses the apoptosis of hippocampal neurons treated with KTM.



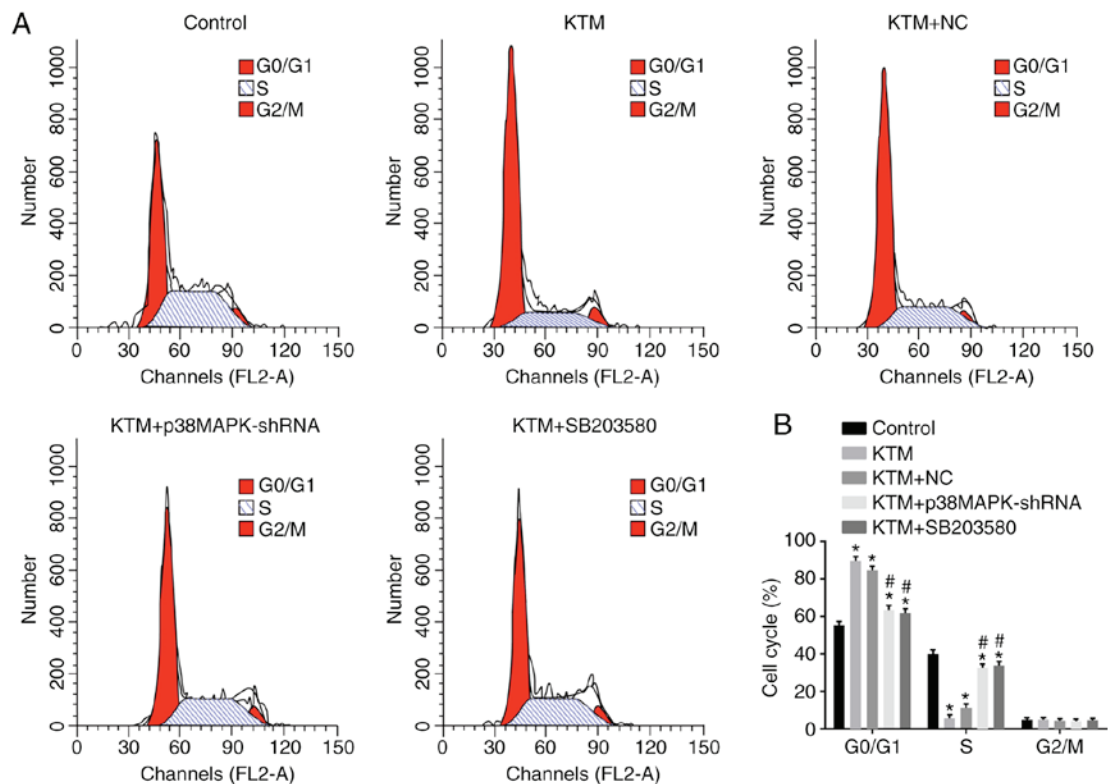


Figure 5. (A and B) Flow cytometry with PI staining demonstrates that silencing p38MAPK facilitates cell cycle progression of hippocampal neurons. \* $P < 0.05$  vs. the control group; # $P < 0.05$  vs. the KTM group. KTM, ketamine; NC, negative control; p38MAPK, p38 mitogen-activated protein kinase; shRNA, short hairpin RNA; PI, propidium iodide.

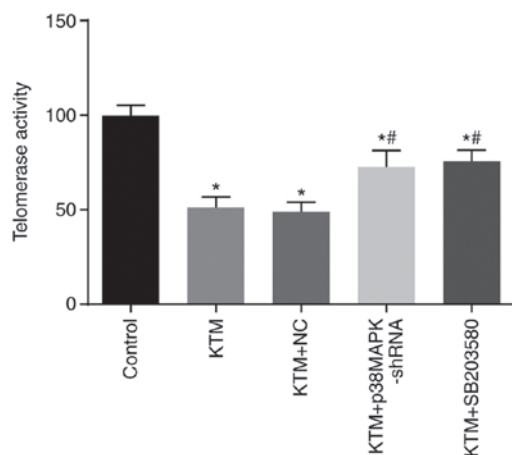


Figure 6. Enzyme-linked immunosorbent assay indicates that silencing p38MAPK promotes the telomerase activity of hippocampal neurons. \* $P < 0.05$  vs. the control group; # $P < 0.05$  vs. the KTM group. KTM, ketamine; NC, negative control; p38MAPK, p38 mitogen-activated protein kinase; shRNA, short hairpin RNA.

## Discussion

KTM serves as the first choice of anesthetic drug for injury caused by natural disaster due to its action on the elevation of cardiac output and blood pressure (6,8). However, KTM has been reported to induce apoptosis of neural stem cells (22) and to have adverse impacts on the hippocampus, promoting neuronal apoptosis through a mitochondrial pathway (15,23). Inhibition of the activation of p38MAPK is a possible protec-

tive mechanism against neuronal injury induced by cerebral ischemia-reperfusion (24). To reduce neuronal apoptosis, the present study investigated the modulatory effect of p38MAPK on KTM-induced apoptosis of rat hippocampal neurons. It was verified that p38MAPK gene silencing is able to block KTM-induced apoptosis of rat hippocampal neurons, which is of great significance for alleviating the symptoms induced by KTM.

Initially, the results of the current study revealed that apoptosis of neurons in KTM-treated groups increased and cell activity decreased. KTM, as a channel blocker of N-methyl-D-aspartate (NMDA) receptors, is widely used as a pediatric anesthetic and is involved in increasing neuronal toxicity in the developing brain (25,26). However, due to the involvement of compensatory upregulated NMDA receptors, KTM at a high concentration may lead to brain cell apoptosis (25). In addition, a study reported that sublethal spinal KTM administration caused neuronal apoptosis of rat pups (27). It has also been demonstrated that KTM was able to prevent the activity of thalamic neurons in rats (28). All these findings are consistent with the observations of the present study.

The current results also demonstrated that the expression of p38MAPK and the extent of p38MAPK phosphorylation increased in hippocampal neurons, and the downregulation of this expression inhibited neuronal apoptosis. Accumulating evidence has indicated the protective effects of silencing p38MAPK against hippocampal apoptosis (29-31). Mammalian p38MAPK is activated by a wide array of cell stressors and is responsive to inflammatory cytokines (32). The p38MAPK is

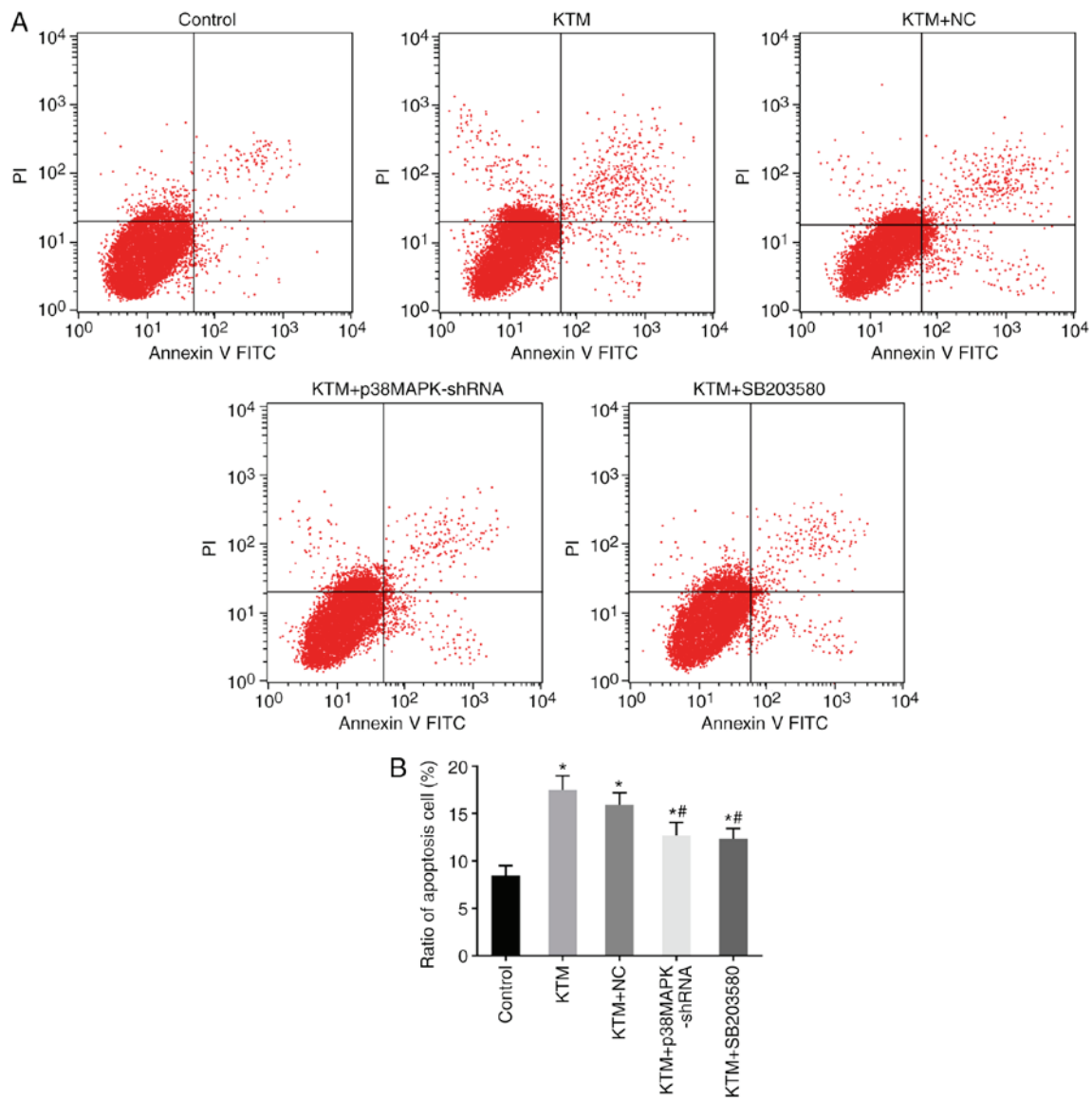


Figure 7. Flow cytometry with Annexin V-FITC/PI staining demonstrates that silencing p38MAPK inhibits the apoptosis of hippocampal neurons. (A) Cell apoptosis in each group observed under a microscope. (B) Cell apoptosis rate in each group. \* $P < 0.05$  vs. the control groups; # $P < 0.05$  vs. the KTM group. KTM, ketamine; NC, negative control; p38MAPK, p38 mitogen-activated protein kinase; shRNA, short hairpin RNA; FITC, fluorescein isothiocyanate; PI, propidium iodide.

also upregulated in certain diseases. For instance, sustained activation of the p38MAPK signaling pathway in muscle stem cells as a result of aging can cause damage to muscle regeneration (17). Certain subtypes of p38MAPK may serve a pro-oncogenic role in cancer (32). Silencing p38MAPK was found to promote the telomerase activity of hippocampal neurons in the current study. It has previously been reported that inhibitors of p38MAPK can be useful in the prevention and treatment of hypoxia-induced neuronal injury (33), which is also consistent with the present study.

Finally, the results of the current study revealed that silencing p38MAPK in hippocampal neurons downregulated the expression of the pro-apoptotic gene Bax and upregulated the expression levels of caspase-3 and apoptosis-suppressing gene Bcl-2 subsequent to treatment with KTM. Liu *et al* (34) previously revealed a significant elevation in the transcriptional activity of the caspase-3 gene during neuronal apoptosis. Other studies have reported that p38MAPK can regulate caspase-3

in several cell lines (35,36). Apart from these findings, p38MAPK activity has been proven to serve a critical role in cell death mediated by nitric oxide in neurons by stimulating Bax translocation to the mitochondria and then activating the cell death pathway (37). Bax is a pro-apoptotic protein that regulates programmed cell death, and its activation causes an increase in outer membrane permeabilization of mitochondria, which finally results in apoptotic cascade events (38). For instance, during the process of sorbitol-induced apoptosis, sorbitol leads to increased levels of Bax in response to p38MAPK signaling (39). By contrast, Bcl-2 rescues cells from apoptosis (40). As an anti-apoptotic factor, Bcl-2 can be phosphorylated by p38MAPK, which regulates the anti-apoptotic role of Bcl-2 (41,42). Furthermore, activation of p38MAPK under stress conditions is a key event in the early induction of apoptosis (42). Thus, the ratio of Bax and Bcl-2 contributes to cellular apoptosis (38). These findings further verify that silencing p38MAPK suppresses the KTM-induced



hippocampal neuron apoptosis by decreasing Bax and caspase-3 expression levels, and elevating the expression of Bcl-2.

In conclusion, the data of the present study revealed that lenti-virus-mediated p38MAPK gene silencing rescued KTM-induced apoptosis of rat hippocampal neurons. Although further experiments are necessary to confirm these results, the findings of the current study are believed to have a significant implication for identifying potential therapeutic strategies in the treatment of apoptosis induced by KTM in hippocampal neurons.

## Acknowledgements

The authors would like to express their sincere appreciation to the reviewers for their critical comments on this article.

## Funding

Not applicable.

## Availability of data and materials

The analyzed datasets generated during the study are available from the corresponding author on reasonable request.

## Authors' contributions

XQG, YLC, LZ and XZ made substantial contributions to the design of the present study. YLC, ZRY and WMC collated the data, and designed and developed the data in the manuscript. YLC and LZ performed data analyses and produced the initial draft of the manuscript. All authors have read and approved the final submitted manuscript.

## Ethics approval and consent to participate

All animal experimentation was approved by the Animal Ethics Committee of Jining No. 1 People's Hospital (Jining, China) and abided by relevant protocols.

## Patient consent for publication

Not applicable.

## Competing interests

The authors declare that they have no competing interests.

## References

- Morgan CJ and Curran HV: Independent Scientific Committee on Drugs: Ketamine use: A review. *Addiction* 107: 27-38, 2012.
- Marland S, Ellerton J, Andolfatto G, Strapazzon G, Thomassen O, Brandner B, Weatherall A and Paal P: Ketamine: Use in anesthesia. *CNS Neurosci Ther* 19: 381-389, 2013.
- Jansen KL: A review of the nonmedical use of ketamine: Use, users and consequences. *J Psychoactive Drugs* 32: 419-433, 2000.
- Bovill JG: Intravenous anesthesia for the patient with left ventricular dysfunction. *Semin Cardiothorac Vasc Anesth* 10: 43-48, 2006.
- Missair A, Pretto EA, Visan A, Lobo L, Paula F, Castillo-Pedraza C, Cooper L and Gebhard RE: A matter of life or limb? A review of traumatic injury patterns and anesthesia techniques for disaster relief after major earthquakes. *Anesth Analg* 117: 934-941, 2013.
- Noh HJ, Bae YM, Park SH, Kim JG, Kim B, Kim YS, Kim SH, Cho SI and Woo NS: The vasodilatory effect of ketamine is independent of the N-methyl-D-aspartate receptor: Lack of functional N-methyl-D-aspartate receptors in rat mesenteric artery smooth muscle. *Eur J Anaesthesiol* 26: 676-682, 2009.
- Mulvey JM, Qadri AA and Maqsood MA: Earthquake injuries and the use of ketamine for surgical procedures: The Kashmir experience. *Anaesth Intensive Care* 34: 489-494, 2006.
- Mulvey JM, Awan SU, Qadri AA and Maqsood MA: Profile of injuries arising from the 2005 Kashmir earthquake: The first 72 h. *Injury* 39: 554-560, 2008.
- Slikker W Jr, Zou X, Hotchkiss CE, Divine RL, Sadovova N, Twaddle NC, Doerge DR, Scallet AC, Patterson TA, Hanig JP, *et al*: Ketamine-induced neuronal cell death in the perinatal rhesus monkey. *Toxicol Sci* 98: 145-158, 2007.
- Scallet AC, Schmued LC, Slikker W Jr, Grunberg N, Faustino PJ, Davis H, Lester D, Pine PS, Sistare F and Hanig JP: Developmental neurotoxicity of ketamine: Morphometric confirmation, exposure parameters, and multiple fluorescent labeling of apoptotic neurons. *Toxicol Sci* 81: 364-370, 2004.
- Tozuka Y, Fukuda S, Namba T, Seki T and Hisatsune T: GABAergic excitation promotes neuronal differentiation in adult hippocampal progenitor cells. *Neuron* 47: 803-815, 2005.
- Jiang XL, Du BX, Chen J, Liu L, Shao WB and Song J: MicroRNA-34a negatively regulates anesthesia-induced hippocampal apoptosis and memory impairment through FGFR1. *Int J Clin Exp Pathol* 7: 6760-6767, 2014.
- Liu B, Zhang H, Xu C, Yang G, Tao J, Huang J, Wu J, Duan X, Cao Y and Dong J: Neuroprotective effects of icariin on corticosterone-induced apoptosis in primary cultured rat hippocampal neurons. *Brain Res* 1375: 59-67, 2011.
- Ko IG, Shin MS, Kim BK, Kim SE, Sung YH, Kim TS, Shin MC, Cho HJ, Kim SC, Kim SH, *et al*: Tadalafil improves short-term memory by suppressing ischemia-induced apoptosis of hippocampal neuronal cells in gerbils. *Pharmacol Biochem Behav* 91: 629-635, 2009.
- Reus GZ, Vieira FG, Abelaire HM, Michels M, Tomaz DB, dos Santos MA, Carlessi AS, Neotti MV, Matias BI, Luz JR, *et al*: MAPK signaling correlates with the antidepressant effects of ketamine. *J Psychiatr Res* 55: 15-21, 2014.
- Rigon AP, Cordova FM, Oliveira CS, Posser T, Costa AP, Silva IG, Santos DA, Rossi FM, Rocha JB and Leal RB: Neurotoxicity of cadmium on immature hippocampus and a neuroprotective role for p38 MAPK. *Neurotoxicology* 29: 727-734, 2008.
- Segalés J, Perdiguer E and Muñoz-Cánoves P: Regulation of muscle stem cell functions: A focus on the p38 MAPK signaling pathway. *Front Cell Dev Biol* 4: 91, 2016.
- Liu XW, Ji EF, He P, Xing RX, Tian BX and Li XD: Protective effects of the p38 MAPK inhibitor SB203580 on NMDA-induced injury in primary cerebral cortical neurons. *Mol Med Rep* 10: 1942-1948, 2014.
- Lu HW, He GN, Ma H and Wang JK: Ketamine reduces inducible superoxide generation in human neutrophils in vitro by modulating the p38 mitogen-activated protein kinase (MAPK)-mediated pathway. *Clin Exp Immunol* 160: 450-456, 2010.
- Tuo YL, Li XM and Luo J: Long noncoding RNA UCA1 modulates breast cancer cell growth and apoptosis through decreasing tumor suppressive miR-143. *Eur Rev Med Pharmacol Sci* 19: 3403-3411, 2015.
- Livak KJ and Schmittgen TD: Analysis of relative gene expression data using real-time quantitative PCR and the 2<sup>-ΔΔCT</sup> method. *Methods* 25: 402-408, 2001.
- Mansouri S, Agartz I, Ögren SO, Patrone C and Lundberg M: PACAP protects adult neural stem cells from the neurotoxic effect of ketamine associated with decreased apoptosis, ER stress and mTOR pathway activation. *PLoS One* 12: e0170496, 2017.
- Bai X, Yan Y, Canfield S, Muravyeva MY, Kikuchi C, Zaja I, Corbett JA and Bosnjak ZJ: Ketamine enhances human neural stem cell proliferation and induces neuronal apoptosis via reactive oxygen species-mediated mitochondrial pathway. *Anesth Analg* 116: 869-880, 2013.
- Zheng GY, Chen XC, Du J, Liu CY, Fang F, Zhang J, Huang TW and Zeng YQ: Inhibitory action of propyl gallate on the activation of SAPK/JNK and p38MAPK induced by cerebral ischemia-reperfusion in rats. *Yao Xue Xue Bao* 41: 548-554, 2006 (In Chinese).
- Zou X, Patterson TA, Divine RL, Sadovova N, Zhang X, Hanig JP, Paule MG, Slikker W Jr and Wang C: Prolonged exposure to ketamine increases neurodegeneration in the developing monkey brain. *Int J Dev Neurosci* 27: 727-731, 2009.

26. Wang C, Sadovova N, Fu X, Schmued L, Scallet A, Hanig J and Slikker W: The role of the *N*-methyl-D-aspartate receptor in ketamine-induced apoptosis in rat forebrain culture. *Neuroscience* 132: 967-977, 2005.
27. Engelhardt T, Blaylock M and Weiss M: Sublethal spinal ketamine produces neuronal apoptosis in rat pups. *Anesthesiology* 114: 718-721, 2011.
28. Foraster MA, Celada P, Jensen AA, Plath N, Herrik KF and Artigas F: P.2.010 Ketamine inhibits the activity of thalamic neurons in anesthetized rats. *Eur Neuropsychopharmacol* 26 (Suppl 1): S31-S32, 2016.
29. Yang S, Zhou G, Liu H, Zhang B, Li J, Cui R and Du Y: Protective effects of p38 MAPK inhibitor SB202190 against hippocampal apoptosis and spatial learning and memory deficits in a rat model of vascular dementia. *Biomed Res Int* 2013: 215798, 2013.
30. Miskovic M, Lalic T, Radivojevic D, Cirkovic S, Vlahovic G, Zamurovic D and Guc-Scekic M: Lower incidence of deletions in the survival of motor neuron gene and the neuronal apoptosis inhibitory protein gene in children with spinal muscular atrophy from Serbia. *Tohoku J Exp Med* 225: 153-159, 2011.
31. Cardaci S, Filomeni G, Rotilio G and Ciriolo MR: p38<sup>MAPK</sup>/p53 signalling axis mediates neuronal apoptosis in response to tetra-hydrobiopterin-induced oxidative stress and glucose uptake inhibition: Implication for neurodegeneration. *Biochem J* 430: 439-451, 2010.
32. Cuenda A and Rousseau S: p38 MAP-kinases pathway regulation, function and role in human diseases. *Biochim Biophys Acta* 1773: 1358-1375, 2007.
33. Lan A, Liao X, Mo L, Yang C, Yang Z, Wang X, Hu F, Chen P, Feng J, Zheng D and Xiao L: Hydrogen sulfide protects against chemical hypoxia-induced injury by inhibiting ROS-activated ERK1/2 and p38MAPK signaling pathways in PC12 cells. *PLoS One* 6: e25921, 2011.
34. Liu W, Wang G and Yakovlev AG: Identification and functional analysis of the rat caspase-3 gene promoter. *J Biol Chem* 277: 8273-8278, 2002.
35. Ohta T, Eguchi R, Suzuki A, Miyakaze S, Ayuzawa R and Kaji K: Hypoxia-induced apoptosis and tube breakdown are regulated by p38 MAPK but not by caspase cascade in an in vitro capillary model composed of human endothelial cells. *J Cell Physiol* 211: 673-681, 2007.
36. Fan Y, Chen H, Qiao B, Luo L, Ma H, Li H, Jiang J, Niu D and Yin Z: Opposing effects of ERK and p38 MAP kinases on HeLa cell apoptosis induced by dipyrithione. *Mol Cells* 23: 30-38, 2007.
37. Ghatan S, Larner S, Kinoshita Y, Hetman M, Patel L, Xia Z, Youle RJ and Morrison RS: p38 MAP kinase mediates bax translocation in nitric oxide-induced apoptosis in neurons. *J Cell Biol* 150: 335-347, 2000.
38. Zhang X, Bi L, Ye Y and Chen J: Formononetin induces apoptosis in PC-3 prostate cancer cells through enhancing the Bax/Bcl-2 ratios and regulating the p38/Akt pathway. *Nutr Cancer* 66: 656-661, 2014.
39. Lu X, Li C, Wang YK, Jiang K and Gai XD: Sorbitol induces apoptosis of human colorectal cancer cells via p38 MAPK signal transduction. *Oncol Lett* 7: 1992-1996, 2014.
40. Huang H, Chan H, Wang YY, Ouyang DY, Zheng YT and Tam SC: Trichosanthin suppresses the elevation of p38 MAPK, and Bcl-2 induced by HSV-1 infection in Vero cells. *Life Sci* 79: 1287-1292, 2006.
41. Torcia M, De Chiara G, Nencioni L, Ammendola S, Labardi D, Lucibello M, Rosini P, Marlier LN, Bonini P, Dello Sbarba P, *et al*: Nerve growth factor inhibits apoptosis in memory B lymphocytes via inactivation of p38 MAPK, prevention of Bcl-2 phosphorylation, and cytochrome c release. *J Biol Chem* 276: 39027-39036, 2001.
42. De Chiara G, Marcocci ME, Torcia M, Lucibello M, Rosini P, Bonini P, Higashimoto Y, Damonte G, Armirotti A, Amodei S, *et al*: Bcl-2 Phosphorylation by p38 MAPK: Identification of target sites and biologic consequences. *J Biol Chem* 281: 21353-21361, 2006.



This work is licensed under a Creative Commons Attribution-NonCommercial-NoDerivatives 4.0 International (CC BY-NC-ND 4.0) License.